

Isolated Channel Vision Transformers: From Single-Channel Pretraining to Multi-Channel Finetuning

Wenyi Lian¹

wenyi.lian@it.uu.se

Patrick Micke²

patrick.micke@igp.uu.se

Joakim Lindblad¹

joakim.lindblad@it.uu.se

Nataša Sladoje¹

natasla.sladoje@it.uu.se

¹ Department of Information Technology
Uppsala University
Uppsala, Sweden

² Department of Immunology, Genetics
and Pathology
Uppsala University
Uppsala, Sweden

Abstract

Vision Transformers (ViTs) have achieved remarkable success in standard RGB image analysis. However, applying ViTs to multi-channel imaging (MCI) data, *e.g.*, for medical and remote sensing applications, remains a challenge. In particular, MCI data often consist of layers acquired from different modalities. Directly training ViTs on such data can obscure modality/channel-specific information and impair performance. In this paper, we propose *Isolated Channel ViT (IC-ViT)*, a simple yet effective training framework for large-scale MCI data. By randomly sampling one channel per image per iteration, IC-ViT learns channel-specific representations without requiring multi-channel fusion during pretraining. These representations are later integrated during finetuning to capture cross-channel dependencies in downstream tasks. Experiments on various benchmarks, including JUMP-CP and CHAMMI for cell microscopy, and So2Sat-LCZ42 for satellite imaging, show the proposed IC-ViT outperforms existing channel-adaptive approaches by 4–14%. Moreover, its efficient training makes it a suitable candidate for large-scale pretraining of foundation models on heterogeneous data. Our code is available at <https://github.com/shermanlian/IC-ViT>.

Introduction

Self-supervised learning (SSL) of Vision Transformers (ViTs), as demonstrated by methods like DINO [6] and DINOv2 [23], has shown clear advantages [1, 23, 34] in learning generalizable representations. The application of an SSL model typically consists of two stages: (1) pretraining on large-scale unlabeled data to learn general representations; and (2) fine-tuning on downstream datasets to address specific, task-oriented problems [11, 35]. However, a key limitation of ViT-based SSL models is that, in both pretraining and fine-tuning stages, they are typically designed for standard RGB images and cannot naturally handle inputs with

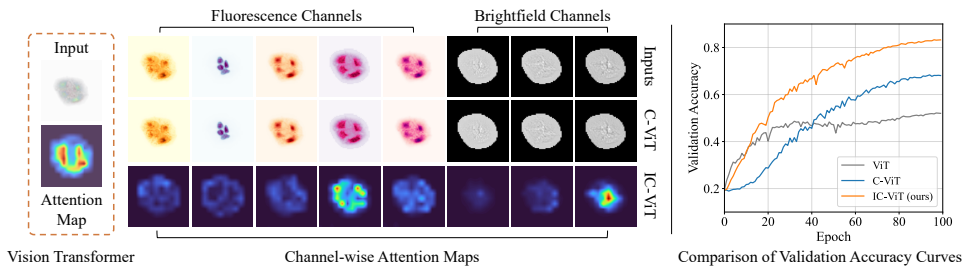


Figure 1: **Left:** Visualization of the attention maps generated from the standard Vision Transformer (ViT) [9], ChannelViT (C-ViT) [10], and the proposed Isolated Channel ViT (IC-ViT). Note that ViT comprises all channels into one patch token while ChannelViT and IC-ViT generate patch tokens for each channel individually. Our IC-ViT tends to extract information from both fluorescence and brightfield channels, while the latter is often ignored by ChannelViT. **Right:** Performance comparison on the JUMP-CP validation dataset [6].

more than three channels or heterogeneous channel configurations, as commonly encountered in multi-channel imaging (MCI) [4].

A common strategy to address this challenge is to finetune large-scale pretrained ViTs on MCI data, typically by modifying the patch embedding layer to accommodate the varying number of input channels. However, directly transferring ViTs pretrained on RGB data to multi-modal MCI datasets often leads to mismatches in input representation [8], resulting in suboptimal exploitation of the available multi-channel information [15]. Recent works have thus shifted focus toward modifying the ViT architecture to support multi-channel inputs [2, 3, 7, 24, 26]. These approaches, commonly referred to as *channel-adaptive ViTs*, extract embeddings independently from each input channel and concatenate them into a single sequence to preserve channel-specific information. However, this expansion in sequence length substantially raises computational costs and significantly prolongs training time, posing a critical challenge in large-scale self-supervised learning [9].

In this paper, we present **Isolated Channel ViT (IC-ViT)**, a simple yet effective self-supervised learning method tailored for multi-channel imaging data. Specifically, IC-ViT is pretrained by learning representations from only a single channel per image at each iteration, rather than relying on all channels simultaneously. This isolated-channel strategy significantly reduces the computational cost of pretraining while enabling effective adaptation to multi-channel downstream tasks. While pretraining focuses on single-channel representations, fine-tuning on downstream tasks allows IC-ViT to integrate information across channels, leading to significantly better task performance.

As illustrated in Figure 1 (left), the attention maps generated by IC-ViT for an eight-channel JUMP-CP microscopy image indicate the model’s ability to capture informative features from both modalities. In addition, the comparison of training curves in the right panel of Figure 1 further confirms its effectiveness for downstream classification. Moreover, the scalability of IC-ViT to large-scale MCI datasets with diverse channel and modality compositions underscores its potential as a foundation model for MCI applications.

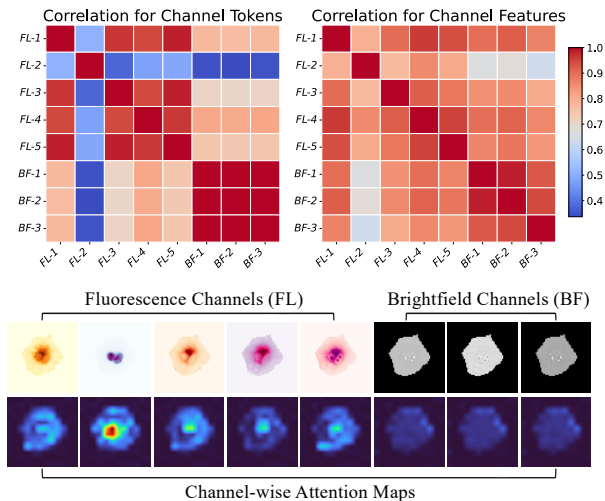


Figure 2: Inter-channel correlation analysis on the JUMP-CP dataset [16]. **Top:** Pairwise correlations of channel tokens and features across eight microscopy channels. **Bottom:** Example of a multi-channel microscopy image and its channel-wise attention maps, obtained from a ViT pretrained with DINO on single-channel inputs.

2 Related work

While ViTs [9] have been highly successful, they have mainly been applied to RGB images [13, 29]. However, multi-channel imaging is finding increased use in many fields, since it captures richer information beyond traditional RGB [17, 19, 20, 22]. This has led to the development of channel-adaptive models for multi-channel data [0, 12, 26]. Recently, ClimaX [21] is presented as a variant of the ViT that employs variable tokenization and aggregation methods to process heterogeneous weather and climate data. DepthwiseViT [2] proposes to process each input channel separately using a depthwise convolution layer. The extracted features are then aggregated by averaging, forming a new representation that is then passed into the ViT backbone. ChannelViT [2] and ChAda-ViT[3] both generate patch tokens independently for each channel and incorporate learnable channel embeddings to explicitly differentiate between channels. Additionally, ChannelViT introduces Hierarchical Channel Sampling (HCS) during training to improve training efficiency. Building upon ChannelViT, DiChaViT [24] further enhances feature diversity by adopting a Diverse Channel Sampling (DCS) strategy. DCS selectively samples less similar channels, reducing redundancy and mitigating over-similarity in channel representations. However, existing channel-adaptive methods suffer from high computational costs due to channel-to-sequence expansion.

3 Method

Multi-channel images often consist of layers acquired through different imaging protocols or modalities. A random example of an eight-channel image from the JUMP-CP dataset, including both fluorescence and brightfield microscopy channels, is shown at the bottom of Figure 2. These layers typically contain distinct yet complementary information that

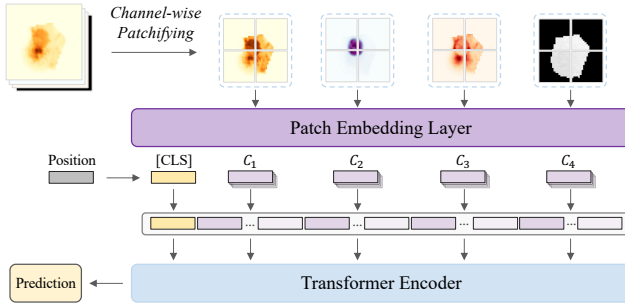


Figure 3: Illustration of channel-wise patchifying in ViT. Each channel is patchified individually, and the resulting patches are embedded into a sequence of vectors, with position and ‘[CLS]’ embeddings added, to form the input to the transformer. C_i denotes the embeddings of the i th channel.

should be jointly leveraged for downstream analysis. In this section, we start from the ViT architecture and study *why* channel-wise patchifying matters for multi-channel images and explore *how* to efficiently extract informative features across channels.

3.1 Channel-wise Patchifying ViT

Preliminary Image patchifying is an important step in all vision transformers which splits the 2D image $\mathbf{x} \in \mathbb{R}^{H \times W \times C}$ into N patches $\mathbf{x}_n \in \mathbb{R}^{P^2 \times C}$, where P is the patch size and $N = HW/P^2$. ViT then maps each image patch into an embedding using a learnable linear projection $\mathbf{W} \in \mathbb{R}^{P^2 C \times D}$ and concatenates all patches as a vector sequence $\mathbf{z} \in \mathbb{R}^{N \times D}$, where D is the embedding dimension. In addition, a position embedding is added to retain positional information and a learnable classification token (‘[CLS]’) embedding is inserted at the start, to serve for final prediction.

Correlation between channels Before introducing the channel-wise patchifying ViT, we examine inter-channel correlations in MCI data. Specifically, we pretrain a single ViT with DINO [9] on single-channel inputs from the JUMP-CP microscopy dataset [6] for self-supervised representation learning. The results are illustrated at the top of Figure 2, showing pairwise correlations of patch tokens and learned channel features across the eight channels in JUMP-CP.

We observe that tokens from fluorescence (FL) and brightfield (BF) channels exhibit lower correlations than tokens within the same modality, indicating that the two modalities provide complementary information. The high correlation observed among brightfield channels is largely due to their nearly identical visual appearance, which naïve token fusion cannot effectively differentiate. By isolating channels during pretraining, it is possible to extract subtle yet discriminative features from visually redundant channels, leading to more informative representations for downstream tasks. In contrast, projecting all channels into a single embedding is akin to “early fusion” in multimodal networks [25], an approach that has been shown to be ineffective in many multimodal learning tasks [15, 16, 18]. Compared to patch tokens, the learned channel features exhibit stronger cross-modality correlations, suggesting that the model effectively learns shared representations bridging FL and BF channels.

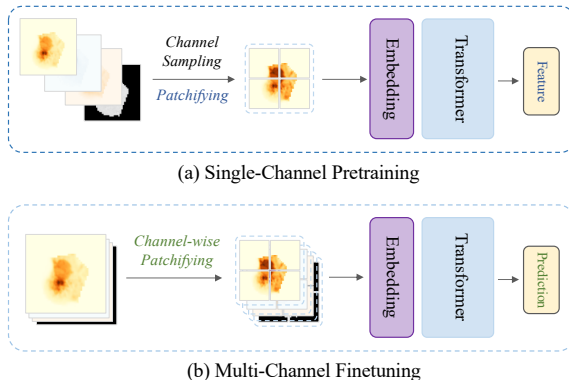


Figure 4: (a) Single-channel pretraining combined. (b) Multi-channel finetuning framework. IC-ViT samples single channel images for pretraining and uses all channels for prediction.

The attention maps in Figure 2 (bottom) further confirm that the model attends to both FL and BF channels. These observations show the effectiveness of isolated-channel training and motivate channel-wise patchifying as a natural solution for multi-channel imaging [4, 24].

Channel-wise patchifying The main idea of channel-wise patchifying is to split the image into multiple single-channel images and patchify these images individually. The same projection layer is used for all channels. After projection, all channel patch embeddings are concatenated as the input sequence to the transformer. An overview of this process is shown in Figure 3. The resulting sequence $\tilde{\mathbf{z}} \in \mathbb{R}^{NC \times D}$ captures information from all channels and is C times longer than the sequence in the original ViT. Moreover, a learnable channel embedding is often added to indicate the spatial index of each channel, similar to the position embedding in ViT [4]. The transformer encoder then leverages self-attention to capture dependencies across patches and channels, yielding more robust feature representations.

3.2 Efficient Multi-Channel Pretraining

We have demonstrated the importance of channel-wise patchifying in Sec. 3.1 and illustrated the effectiveness of feature extraction with DINO pretraining in Figure 2. However, as noted earlier, channel-wise patchifying extends the sequence length by C times, thereby leading to a quadratic growth in computational cost with respect to the number of channels due to the self-attention mechanism. This significantly limits the scalability of pretraining, particularly for self-supervised methods such as DINO [6] and DINOv2 [23], which process multiple augmented views per iteration and require dual networks (teacher and student) throughout training.

Single-channel pretraining Training ViTs on individual channels, as described in Sec. 3.1, has empirically shown the ability to extract informative channel representations. Since channel-wise patchifying introduces no channel-specific parameters, the number of channels can be adapted without modifying the network architecture (ViT naturally supports variable sequence lengths). Then, the ViT pretrained on the individual channels can be finetuned on multi-channel images (MCI) for a downstream task. We refer to this approach as Isolated

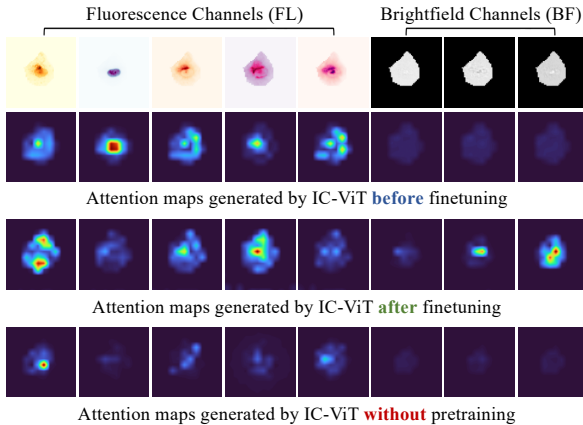


Figure 5: Attention maps on an eight-channel microscopy image from JUMP-CP dataset [6], generated by IC-ViT under different training settings: pretraining only (top), after supervised fine-tuning (middle), and trained directly with labels without pretraining (bottom).

Channel ViT (IC-ViT). It is highly efficient for MCI pretraining and facilitates transfer to downstream tasks. An overview of the framework is presented in Figure 4. In the pretraining stage, one channel is randomly sampled from each image and patchified as in a standard ViT for single-channel (grayscale) inputs. DINO [5] is employed to learn self-supervised representations from individual channels. During fine-tuning, channel-wise patchifying is applied to all channels simultaneously to leverage global cross-channel information.

Figure 5 illustrates the attention maps of IC-ViT under different training settings. Across all cases, the model attends more strongly to fluorescence channels, which typically contain clearer and more discriminative information than brightfield channels. Pretraining enables the model to also capture structural information from brightfield channels, which becomes better integrated with fluorescence features after finetuning. In contrast, models trained directly from scratch fail to adequately attend to brightfield channels, resulting in inferior performance compared to the finetuned model. Further details are provided in Sec. 4.

MCI foundation models With its efficient pretraining and finetuning scheme, the proposed IC-ViT is scalable to large MCI datasets with diverse channels and modalities. A key challenge in training models on multimodal multi-channel datasets is the difficulty of unifying heterogeneous image channels within the same training batch, which is required by most deep learning frameworks. Existing solutions typically adopt either (1) padding all images along the channel dimension, analogous to sentence padding in language models [27], or (2) performing separate forward passes for different channel batches followed by gradient aggregation for parameter updates [24]. However, both approaches are rigid and constrained by variability in channel numbers. In contrast, IC-ViT addresses this challenge by sampling a single channel from each image at a time, thereby ensuring channel uniformity within the batch while maintaining training efficiency.

4 Experiments

In this section, we evaluate the proposed IC-ViT method on various tasks and MCI datasets.

Model	CHAMMI [10]			JUMP-CP [8]		So2Sat [16]	
	WTC	HPA	Avg F1-score	Full	Partial	Full	Partial
DepthwiseViT [10]	50.35	71.52	60.94	49.86	44.98	60.41	43.41
TemplateMixingViT [16]	49.51	64.52	57.02	52.48	43.85	55.86	37.28
HyperNetViT [12]	45.17	63.90	54.54	47.07	42.43	60.73	41.88
ChAda-ViT [3]	67.08	60.67	63.88	65.03	42.15	56.98	12.38
ChannelViT [10]	67.66	62.14	64.90	67.51	56.49	61.03	46.16
DiChaViT [24]	73.36	63.35	68.36	69.19	57.98	63.36	47.76
IC-ViT (Ours)	74.45	70.76	72.54	83.43	66.01	67.10	48.21

Table 1: Comparison of method performance on test sets of three multi-channel image benchmarks: CHAMMI, JUMP-CP, and So2Sat. Best scores are shown in **bold**.

4.1 Datasets and Implementation

We evaluate IC-ViT on three publicly available multi-channel benchmarks from the medical and remote sensing domains:

1) *JUMP-CP* [8], a widely used benchmark for cell microscopy imaging, with each image captured across eight channels (five fluorescence and three brightfield). Following previous works [10, 24], we use the compound perturbation plate ‘BR00116991’, which comprises 127K training images, 45K validation images, and 45K test images.

2) *CHAMMI* [10], a microscopy benchmark for channel-invariant models which combines three multi-channel imaging datasets with varying channel counts: WTC-11 hiPSC (WTC-11, 3 channels, 65K images) [30], Human Protein Atlas (HPA, 4 channels, 67K images) [30], and Cell Painting (CP, 5 channels, 88K images) [32].

3) *So2Sat-LCZ42* [16], a remote sensing dataset consisting of Sentinel-1 (8 radar channels) and Sentinel-2 (10 multispectral channels) imagery, with 352K training images, 24K validation images, and 24K test images.

We apply the proposed single-channel sampling strategy for pretraining in all tasks. During both pretraining and fine-tuning, only the training data are used. For fine-tuning, we follow the same experimental setup as ChannelViT [10] and DiChaViT [24] to ensure fair comparison. For example, we use cross-entropy loss for JUMP-CP and So2Sat, and proxy-based loss [23] for CHAMMI. For all downstream tasks, we employ the AdamW optimizer with a learning rate schedule that starts with a warm-up phase for the first 10 epochs.

For both JUMP-CP and So2Sat, the epoch achieving the highest validation accuracy is chosen, and the test set performance of that checkpoint is reported as the final top-1 accuracy. For CHAMMI, we follow the official CHAMMI evaluation protocol [10], using the final checkpoint and reporting macro-F1 scores. Please refer to the Supplementary Materials for additional details on datasets, training settings, and results.

4.2 Results

We compare the proposed IC-ViT to the following state-of-the-art channel-adaptive approaches: DepthwiseViT [10], TemplateMixingViT [16], HyperNetViT [12], ChAda-ViT [3], ChannelViT [10], and DiChaViT [24]. For fairness, IC-ViT and all baseline methods are trained under the same experimental protocol, with identical task objectives, loss functions, and training splits. Importantly, IC-ViT employs the same number of parameters as ChannelViT, ensuring that performance differences are attributable to training strategies rather than model capacity.

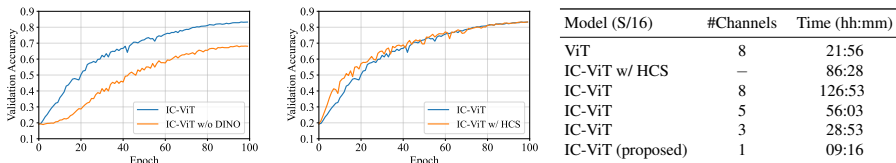


Figure 6: (Left:) Validation accuracy for IC-ViT vs. IC-ViT without DINO pretraining. (Middle) Training curves of IC-ViT and its variant using HCS strategy [2]. (Right:) Pre-training time (in hours:minutes) across different models and channel configurations on the JUMP-CP training set. Batch sizes are adjusted based on the available memory. The number of channels in “IC-ViT w/ HCS” is dynamically selected (denoted with “—”).

The quantitative results are reported in Table 1. For the JUMP-CP and So2Sat datasets, our evaluations cover two practical scenarios: (1) training and testing with all channels (denoted as “Full”); and (2) training with all, but testing only with a partial set of channels (denoted as “Partial”), simulating situations where only one modality is available at inference (the fluorescence channels for JUMP-CP and the Sentinel-1 channels for So2Sat). It is observed that the proposed IC-ViT consistently outperforms other approaches across most tasks and datasets. On the JUMP-CP dataset, IC-ViT achieves an improvement of 14–16% over ChannelViT and DiChaViT in full-channel settings, and 8–10% in partial-channel settings, demonstrating both its robustness to missing channels and its overall effectiveness. Similarly, on the CHAMMI benchmark, our method surpasses DiChaViT, the second-best method, by 4.18% in overall F1-score, further confirming its strong capability for robust representation learning and generalization.

5 Analysis and Discussion

Effectiveness of self-supervised learning We evaluate the impact of self-supervised pre-training in our method by comparing models trained with and without DINO on the JUMP-CP training set. As shown in Figure 6 (left), the model pretrained with DINO significantly outperforms its supervised-only counterpart in downstream validation accuracy, highlighting the benefits of self-supervised representations.

Impact of channel sampling strategies on pretraining efficiency A major limitation of channel-adaptive approaches is the increased computational cost caused by expanding the channel dimension into the sequence length. We compare the pretraining times of ViT and IC-ViT variants employing different channel sampling strategies on the JUMP-CP training set over 100 epochs. All experiments are conducted on four 80GB A100 GPUs with consistent training configurations, except that the batch size varies with memory usage across channel settings.

As shown in Figure 6 (right), pretraining IC-ViT on all channels (8 channels) without any sampling strategy takes approximately 127 hours (5 days and 7 hours). IC-ViT with Hierarchical Channel Sampling (HCS) instead samples a fixed number of channels at each iteration, thereby exposing the model to more channel information than our single-channel strategy. While incorporating HCS during DINO pretraining reduces the duration to 86 hours (3 days and 14 hours), Bao et al. [2] reported that it can introduce instability into the

#channels	#comb.	ViT	ChannelViT	IC-ViT (Ours)
8	1	56.87	68.09	83.41
7	8	49.35±09.38	61.02±09.78	79.72±06.87
6	28	42.38±10.64	53.45±12.40	72.42±10.11
5	56	35.78±10.18	45.50±13.23	63.40±12.31
4	70	29.84±08.32	37.37±12.25	52.56±13.10
3	56	24.94±05.43	29.68±09.22	40.33±11.71
2	28	21.54±02.37	23.77±04.89	28.80±07.45
1	8	19.92±00.51	20.85±01.64	21.84±02.54

Table 2: Test accuracy on JUMP-CP [9]. ‘#comb.’ denotes the number of $\binom{8}{k}$ combinations of channels. The results of ViT and ChannelViT are reported from their original paper [9].

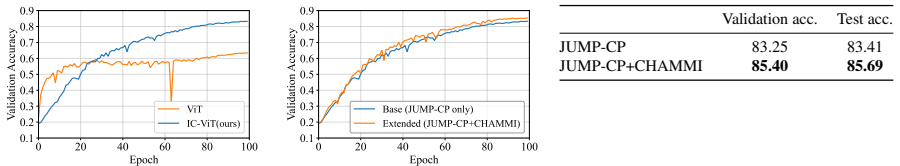


Figure 7: (Left:) Performance curves of IC-ViT and ViT, both pretrained and finetuned on the JUMP-CP dataset. (Middle:) Multi-dataset pretraining evaluation. Validation accuracy curves for the baseline model (pretrained solely on JUMP-CP) and the extended model (pretrained on both JUMP-CP and CHAMMI). The extended pretraining generally results in higher accuracy throughout training. (Right:) Test accuracy at the epoch of highest validation accuracy. Best results in **bold**.

self-distillation objective, which we also observe. More importantly, as shown in Figure 6 (middle), although this variant achieves higher accuracy in the early stages of training, its advantage diminishes over time, resulting in comparable final performance to our method, which achieves similar results with substantially less training time (requiring only 9 hours).

Effectiveness of channel-specific representation learning The standard ViT [9] treats all patches uniformly without differentiating among input channels, thereby neglecting the potentially independent semantic content carried by each channel/modality [9]. We pretrain both ViT and IC-ViT using DINO on the JUMP-CP training set, and subsequently fine-tune them on the same dataset for the downstream classification task. The corresponding training curves are shown in Figure 7 (left). While the standard ViT initially achieves higher accuracy, its performance stagnates after about 10 epochs. In contrast, IC-ViT continues to improve steadily, demonstrating the advantage of channel-specific representation learning.

Robustness evaluation on channel subsets Table 1 shows that IC-ViT outperforms baseline methods even when an entire modality is absent at inference, indicating its potential for handling inputs with missing channels. We further extend this evaluation to scenarios with randomly missing channels by analyzing test accuracy on the JUMP-CP dataset when different subsets of channels are removed during inference. All possible channel combinations are considered, and Table 2 reports the mean and standard deviation across these combinations for different methods.

As illustrated in [Table 2](#), IC-ViT consistently achieves higher average accuracy across different channel subsets, demonstrating strong robustness to partial or missing inputs. Moreover, the steady improvement in accuracy with more available channels indicates that our single-channel sampling strategy effectively leverages independent semantic information from each channel, enhancing the overall feature diversity and informativeness.

Pretraining with extended datasets As discussed in [Sec. 3.2](#), IC-ViT has the potential to serve as a foundation model for MCI tasks by pretraining on extended datasets with a larger variety of multi-channel inputs. To provide a preliminary evaluation of this capability, we compare a baseline IC-ViT model pretrained solely on the JUMP-CP dataset with an extended version pretrained on both JUMP-CP and CHAMMI. Both models are subsequently fine-tuned on the JUMP-CP training set under the same experimental settings. As shown in [Figure 7](#) (middle), the model pretrained on the combined dataset generally leads to higher validation accuracy across most training epochs. As summarized in [Figure 7](#) (right), pretraining with additional data results in over a 2% improvement in both validation and test accuracy, further highlighting the model’s effectiveness for pretraining on heterogeneous multi-channel data.

Limitations and future work While IC-ViT demonstrates strong empirical performance across diverse MCI benchmarks, several limitations remain. First, the single-channel pretraining strategy inevitably neglects inter-channel correlations during representation learning, which may lead to partial information loss, especially in domains with low channel redundancy or high cross-channel dependencies. Second, our current uniform channel sampling treats all channels equally, which could be suboptimal in the presence of noisy or less informative channels. Future work could incorporate adaptive or learnable channel weighting mechanisms to better exploit heterogeneous data. Third, our experiments are limited to DINO-based self-supervised pretraining; extending the framework to other SSL paradigms such as MAE [[12](#)], BYOL [[10](#)], or SimMIM [[63](#)] would further validate its generality. Finally, the evaluation is restricted to microscopy and remote sensing datasets. Broader investigations on other multi-channel modalities, such as RGB-D imaging or medical MRI, will be essential to assess the scalability and universality of IC-ViT.

6 Conclusion

In this study, we tackle the challenge of learning from multi-channel imaging (MCI) data, where input channels often correspond to distinct modalities or measurements. We propose *Isolated Channel Vision Transformer (IC-ViT)*, a simple yet effective framework that performs pretraining on single-channel inputs to learn channel-specific representations, while naturally supporting datasets with varying channel configurations. Upon fine-tuning, IC-ViT integrates complementary information across channels, leading to improved performance on downstream MCI tasks. Through extensive experiments on diverse datasets and tasks, we demonstrate that IC-ViT outperforms existing channel-adaptive approaches. Its efficiency and scalability make it a strong candidate for large-scale pretraining in MCI imaging.

Acknowledgement The computations and data handling were enabled by resources provided by Chalmers e-Commons at Chalmers.

References

- [1] Muhammad Awais, Muzammal Naseer, Salman Khan, Rao Muhammad Anwer, Hisham Cholakkal, Mubarak Shah, Ming-Hsuan Yang, and Fahad Shahbaz Khan. Foundation models defining a new era in vision: a survey and outlook. *IEEE TPAMI*, 2025.
- [2] Yujia Bao, Srinivasan Sivanandan, and Theofanis Karaletsos. Channel vision transformers: An image is worth $1 \times 16 \times 16$ words. In *ICLR*, 2024. URL <https://openreview.net/forum?id=CK5Hfb5hBG>.
- [3] Nicolas Bourrieux, Ihab Bendidi, Ethan Cohen, Gabriel Watkinson, Maxime Sanchez, Guillaume Bollot, and Auguste Genovesio. ChAda-ViT: Channel adaptive attention for joint representation learning of heterogeneous microscopy images. In *CVPR*, pages 11556–11565, 2024.
- [4] Lei Cai, Jingyang Gao, and Di Zhao. A review of the application of deep learning in medical image classification and segmentation. *Annals of Translational Medicine*, 8(11):713, 2020.
- [5] Mathilde Caron, Hugo Touvron, Ishan Misra, Hervé Jégou, Julien Mairal, Piotr Bojanowski, and Armand Joulin. Emerging properties in self-supervised vision transformers. In *ICCV*, pages 9650–9660, 2021.
- [6] Srinivas Niranj Chandrasekaran, Beth A Cimini, Amy Goodale, Lisa Miller, Maria Kost-Alimova, Nasim Jamali, John G Doench, Briana Fritchman, Adam Skepner, Michelle Melanson, et al. Three million images and morphological profiles of cells treated with matched chemical and genetic perturbations. *Nature Methods*, 21(6):1114–1121, 2024.
- [7] Zitong Sam Chen, Chau Pham, Siqi Wang, Michael Doron, Nikita Moshkov, Bryan Plummer, and Juan C Caicedo. CHAMMI: A benchmark for channel-adaptive models in microscopy imaging. *NeurIPS*, 36:19700–19713, 2023.
- [8] Aloïs de La Comble and Ken Prepin. Efficient transfer learning for multi-channel convolutional neural networks. In *2021 17th International Conference on Machine Vision and Applications (MVA)*, pages 1–6. IEEE, 2021.
- [9] Alexey Dosovitskiy, Lucas Beyer, Alexander Kolesnikov, Dirk Weissenborn, Xiaohua Zhai, Thomas Unterthiner, Mostafa Dehghani, Matthias Minderer, Georg Heigold, Sylvain Gelly, Jakob Uszkoreit, and Neil Houlsby. An image is worth 16×16 words: Transformers for image recognition at scale. In *ICLR*, 2021. URL <https://openreview.net/forum?id=YicbFdNTTy>.
- [10] Linus Ericsson, Henry Gouk, Chen Change Loy, and Timothy M Hospedales. Self-supervised representation learning: Introduction, advances, and challenges. *IEEE Signal Processing Magazine*, 39(3):42–62, 2022.
- [11] Jean-Bastien Grill, Florian Strub, Florent Altché, Corentin Tallec, Pierre Richemond, Elena Buchatskaya, Carl Doersch, Bernardo Avila Pires, Zhaohan Guo, Mohammad Gheshlaghi Azar, et al. Bootstrap your own latent—a new approach to self-supervised learning. *Advances in neural information processing systems*, 33:21271–21284, 2020.

- [12] David Ha, Andrew M. Dai, and Quoc V. Le. Hypernetworks. In *ICLR*, 2017. URL <https://openreview.net/forum?id=rkpACellx>.
- [13] Kai Han, Yunhe Wang, Hanting Chen, Xinghao Chen, Jianyuan Guo, Zhenhua Liu, Yehui Tang, An Xiao, Chunjing Xu, Yixing Xu, et al. A survey on vision transformer. *IEEE TPAMI*, 45(1):87–110, 2022.
- [14] Kaiming He, Xinlei Chen, Saining Xie, Yanghao Li, Piotr Dollár, and Ross Girshick. Masked autoencoders are scalable vision learners. In *Proceedings of the IEEE/CVF conference on computer vision and pattern recognition*, pages 16000–16009, 2022.
- [15] Xiaoyu He, Yong Wang, Shuang Zhao, and Xiang Chen. Co-attention fusion network for multimodal skin cancer diagnosis. *Pattern Recognition*, 133:108990, 2023.
- [16] Hamid Reza Vaezi Joze, Amirreza Shaban, Michael L Iuzzolino, and Kazuhito Koishida. Mmtm: Multimodal transfer module for cnn fusion. In *CVPR*, pages 13289–13299, 2020.
- [17] Jae-Hyeok Lee, Sangmin S Lee, Hak Gu Kim, Sa-Kwang Song, Seongchan Kim, and Yong Man Ro. Mcsip net: Multichannel satellite image prediction via deep neural network. *IEEE Transactions on Geoscience and Remote Sensing*, 58(3):2212–2224, 2019.
- [18] Wenyi Lian, Joakim Lindblad, Christina Runow Stark, Jan-Michaél Hirsch, and Nataša Sladoje. Let it shine: Autofluorescence of papanicolaou-stain improves ai-based cytological oral cancer detection. *Computers in Biology and Medicine*, 185:109498, 2025.
- [19] Mingxia Liu, Jun Zhang, Ehsan Adeli, and Dinggang Shen. Deep multi-task multi-channel learning for joint classification and regression of brain status. In *International Conference on Medical Image Computing and Computer-Assisted Intervention*, pages 3–11. Springer, 2017.
- [20] Sampa Misra, Seungwan Jeon, Seiyon Lee, Ravi Managuli, In-Su Jang, and Chulhong Kim. Multi-channel transfer learning of chest x-ray images for screening of covid-19. *Electronics*, 9(9):1388, 2020.
- [21] Tung Nguyen, Johannes Brandstetter, Ashish Kapoor, Jayesh K Gupta, and Aditya Grover. ClimaX: A foundation model for weather and climate. In Andreas Krause, Emma Brunskill, Kyunghyun Cho, Barbara Engelhardt, Sivan Sabato, and Jonathan Scarlett, editors, *Proc. of the 40th International Conference on Machine Learning*, volume 202 of *Proceedings of Machine Learning Research*, pages 25904–25938. PMLR, 23–29 Jul 2023.
- [22] Dong Nie, Junfeng Lu, Han Zhang, Ehsan Adeli, Jun Wang, Zhengda Yu, LuYan Liu, Qian Wang, Jinsong Wu, and Dinggang Shen. Multi-channel 3d deep feature learning for survival time prediction of brain tumor patients using multi-modal neuroimages. *Scientific Reports*, 9(1):1103, 2019.
- [23] Maxime Oquab, Timothée Darcet, Théo Moutakanni, Huy V. Vo, Marc Szafraniec, Vasil Khalidov, Pierre Fernandez, Daniel HAZIZA, Francisco Massa, Alaaeldin El-Nouby, Mido Assran, Nicolas Ballas, Wojciech Galuba, Russell Howes, Po-Yao

- Huang, Shang-Wen Li, Ishan Misra, Michael Rabbat, Vasu Sharma, Gabriel Synnaeve, Hu Xu, Herve Jegou, Julien Mairal, Patrick Labatut, Armand Joulin, and Piotr Bojanowski. DINOv2: Learning robust visual features without supervision. *Transactions on Machine Learning Research*, 2024. ISSN 2835-8856. URL <https://openreview.net/forum?id=a68SUt6zFt>. Featured Certification.
- [24] Chau Pham and Bryan Plummer. Enhancing feature diversity boosts channel-adaptive vision transformers. In A. Globerson, L. Mackey, D. Belgrave, A. Fan, U. Paquet, J. Tomczak, and C. Zhang, editors, *NeurIPS*, volume 37, pages 89782–89805. Curran Associates, Inc., 2024. URL https://proceedings.neurips.cc/paper_files/paper/2024/file/a376fb45a0396c6fbf2f914dce8f7316-Paper-Conference.pdf.
- [25] Dhanesh Ramachandram and Graham W Taylor. Deep multimodal learning: A survey on recent advances and trends. *IEEE Signal Processing Magazine*, 34(6):96–108, 2017.
- [26] Pedro Savarese and Michael Maire. Learning implicitly recurrent CNNs through parameter sharing. In *ICLR*, 2019. URL <https://openreview.net/forum?id=rJgYxn09Fm>.
- [27] Ilya Sutskever, Oriol Vinyals, and Quoc V Le. Sequence to sequence learning with neural networks. *Advances in neural information processing systems*, 27:3104–3112, 2014.
- [28] Eu Wern Teh, Terrance DeVries, and Graham W Taylor. Proxynca++: Revisiting and revitalizing proxy neighborhood component analysis. In *ECCV*, pages 448–464. Springer, 2020.
- [29] Hans Thisanke, Chamli Deshan, Kavindu Chamith, Sachith Seneviratne, Rajith Vidanaarachchi, and Damayanthi Herath. Semantic segmentation using vision transformers: A survey. *Engineering Applications of Artificial Intelligence*, 126:106669, 2023.
- [30] Peter J Thul, Lovisa Åkesson, Mikaela Wiking, Diana Mahdessian, Aikaterini Geladaki, Hammou Ait Blal, Tove Alm, Anna Asplund, Lars Björk, Lisa M Breckels, et al. A subcellular map of the human proteome. *Science*, 356(6340):eaal3321, 2017.
- [31] Matheus P Viana, Jianxu Chen, Theo A Knijnenburg, Ritvik Vasani, Calysta Yan, Joy E Arakaki, Matte Bailey, Ben Berry, Antoine Borensztein, Eva M Brown, et al. Integrated intracellular organization and its variations in human ips cells. *Nature*, 613(7943):345–354, 2023.
- [32] Gregory P Way, Ted Natoli, Adeniyi Adeboye, Lev Litichevskiy, Andrew Yang, Xiaodong Lu, Juan C Caicedo, Beth A Cimini, Kyle Karhohs, David J Logan, et al. Morphology and gene expression profiling provide complementary information for mapping cell state. *Cell Systems*, 13(11):911–923, 2022.
- [33] Zhenda Xie, Zheng Zhang, Yue Cao, Yutong Lin, Jianmin Bao, Zhuliang Yao, Qi Dai, and Han Hu. Simmim: A simple framework for masked image modeling. In *Proceedings of the IEEE/CVF conference on computer vision and pattern recognition*, pages 9653–9663, 2022.

- [34] Hanwen Xu, Naoto Usuyama, Jaspreet Bagga, Sheng Zhang, Rajesh Rao, Tristan Naumann, Cliff Wong, Zelalem Gero, Javier González, Yu Gu, et al. A whole-slide foundation model for digital pathology from real-world data. *Nature*, 630(8015):181–188, 2024.
- [35] Ce Zhou, Qian Li, Chen Li, Jun Yu, Yixin Liu, Guangjing Wang, Kai Zhang, Cheng Ji, Qiben Yan, Lifang He, et al. A comprehensive survey on pretrained foundation models: A history from bert to chatgpt. *International Journal of Machine Learning and Cybernetics*, pages 1–65, 2024.
- [36] XiaoXiang Zhu, Jingliang Hu, Chunping Qiu, Yilei Shi, Jian Kang, Lichao Mou, Hossein Bagheri, Matthias Haberle, Yuansheng Hua, Rong Huang, Lloyd Hughes, Hao Li, Yao Sun, Guichen Zhang, Shiyao Han, Michael Schmitt, and Yuanyuan Wang. So2sat lcz42: A benchmark data set for the classification of global local climate zones [software and data sets]. *IEEE Geoscience and Remote Sensing Magazine*, 8(3):76–89, 2020. doi: 10.1109/MGRS.2020.2964708.